Random depth access full-field heterodyne low-coherence interferometry utilizing acousto-optic modulation and a complementary metal-oxide semiconductor camera

Patrick Egan and Michael J. Connelly

Optical Communications Research Group, University of Limerick, Castletroy, County Limerick, Ireland

Fereydoun Lakestani and Maurice P. Whelan

Photonics Group, Institute for Health and Consumer Protection, European Commission Joint Research Centre, Ispra (VA) I-21020, Italy

Received November 8, 2005; revised December 31, 2005; accepted January 3, 2006; posted January 9, 2006 (Doc. ID 66116)

With analog scanning, time-domain low-coherence interferometry lacks precise depth information, and optical carrier generation demands a linear scanning speed. Full-field heterodyne low-coherence interferometry that uses a logarithmic complementary metal-oxide semiconductor camera, acousto-optic modulation, and digital depth stepping is reported, with which random regions of interest, lateral and axial, can be accessed. Furthermore, nanometer profilometry is possible through heterodyne phase retrieval of the interference signal. The approach demonstrates inexpensive yet high-precision functional machine vision offering true digital random access in three dimensions. © 2006 Optical Society of America

OCIS codes: 040.2840, 120.3180, 150.6910, 230.1040.

In low-coherence interferometry (LCI),[1] typically consisting of a Michelson interferometer with a low-coherence light source, interference is achieved only when the path lengths of the two interferometer arms are matched within the coherence length of the source. If the path length of one arm is linearly scanned, the result is an interference envelope with an optical carrier of maximum amplitude centered at the point of path length matching. Thus depth scanning and optical carrier generation are facilitated in one operation, and profiling is obtained by detection of the intensity envelope.

Decoupling depth scanning from optical carrier generation by use of digital depth stepping and frequency shifting between two interferometer arms (Fig. 1) by acousto-optic modulators (AOMs) offers improved functionality over its analog scanning counterparts in LCI. Random regions of interest (ROIs) can be directly accessed in depth and their precise axial positions known within the resolution of the digital stepper. Furthermore, a high-fidelity optical carrier, generated without electromechanical movement, permits the utilization of full-field interferometric phase measurement inside the coherence gate of the light source. Thus, further to the micrometer depth selectivity of LCI, full-field profilometry on a nanometer scale is achieved within the coherence envelope through phase retrieval of the interferometric signal.

Heterodyne LCI was demonstrated,[2] but the system was single point and used analog depth scanning. A full-field phase-stepping approach to LCI was reported[3]; however, in addition to burdensome calibration procedures, perturbations owing to electromechanical scanning are highly undesirable in nanoscale measurement. The use of differential phase contrast[4] in LCI has furthered the ability of optical coherence tomography[5] to achieve subwavelength cellular measurement. However, phase measurement through heterodyne interferometry offers superior precision and robustness against system temperature drift, vibrations, and random noise.[6]

Previously,[7] this logarithmic complementary metal-oxide semiconductor (CMOS) camera was utilized in full-field LCI with analog depth scanning. The camera features random ROI pixel access in space and time at fast frame rates, and lateral scanning of the sample was implemented by electronic scanning of the pixels of the camera. In this Letter we report the integration of LCI with full-field heterodyne phase retrieval and the achievement of full-field heterodyne LCI offering high resolution, truly random ROI imaging in three dimensions without electromechanical analog scanning.

The optical setup (Fig. 1) utilized a Mach–Zehnder interferometer, with an AOM in each arm slightly rotated off-perpendicular such that the Bragg angle was met. The AOMs were driven at 80 MHz, and their beat frequency, or heterodyning (carrier) frequency f_c, was phase locked to a low-frequency oscillator capable of steady locking from 3 to 1000 Hz. The light source was an 830 nm superluminescent diode (SLD) with a full width at half-maximum bandwidth of 25 nm and supplied 5 mW of power with a collimated beam diameter of approximately 2 mm. The sample (Fig. 2) consisted of two engineering gauge blocks, of heights 1.0 and 1.05 mm, attached to a plane mirror and was illuminated with the first-order diffracted beam from AOM1. The sample was specifically chosen to present the dual functionality of the technique; with approximate knowledge of the sample it was possible to step directly to an esti-

0146-9592/06/070912-3/$15.00

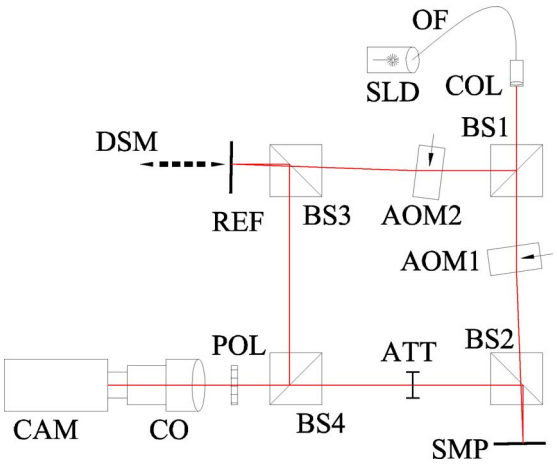

Fig. 1. (Color online) Experimental setup: OF optical fiber; COL, collimating lens; BS1–BS4; 50/50 beam splitters; ATT, variable attenuator; POL, polarizer; DSM, digital stepper motor; CO, camera objective; CAM, CMOS camera; other references defined in text. The reference (REF) was a plane mirror. The sample (SMP) was a polished metal gauge block.

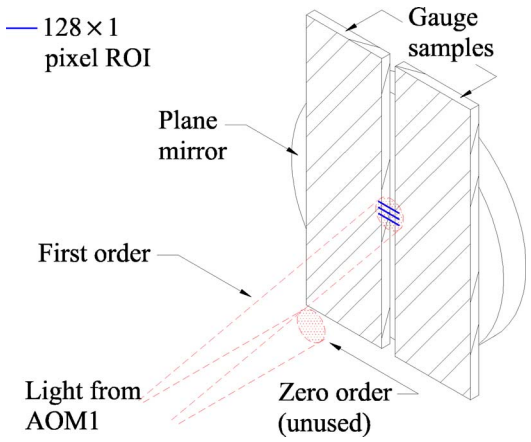

Fig. 2. (Color online) Sample illuminated with a first-order diffracted beam from AOM1.

mated surface location in depth and then step through the coherence envelope. On locating the coherence envelope, we implemented full-field phase retrieval at a fixed position inside.

To demonstrate the micrometer profiling and random lateral and axial access capability of the approach, we simultaneously accessed three 128 $\times$1 pixel ROIs on the camera 1024 times at a rate of 1106 Hz, with f_c=50 Hz. The reference mirror was stepped with a digital stepper motor of 100 nm resolution in 1 μm steps. The coherence envelope detected on a single pixel (Fig. 3) can be presented as discrete values of the light-intensity ac rms, in terms of pixel gray scale levels as the path length is stepped; the interference signal is a cw signal at each fixed position of the digital stepper and use of the ac rms is an effective means of estimating the amplitude of a cw signal while reducing random noise. With approximate preknowledge of the sample it was possible to skip directly to a depth of interest and then step through the coherence envelope (Fig. 4) at each surface.

By stepping the reference arm into the coherence envelope at a fixed position, we implemented phase retrieval of the interferometric signal from each pixel. A 32$\times$32 pixel ROI on the 1.05 mm gauge block was sampled 1024 times at a rate of 431 Hz, with f_c =25 Hz. The intensity signal from each pixel can be represented as

$$s_{xy}(t) = a_{xy}(t) + b_{xy}(t)\cos[2\pi f_c t + \alpha_{xy}(t) + \phi_{xy}], \quad (1)$$

where $a_{xy}(t)$ and $b_{xy}(t)$ take into account light-intensity modulations; $\alpha_{xy}(t)$ is the phase changes that are due to carrier frequency modulation, translational vibrations, and drifts; f_c is the carrier frequency; and ϕ_{xy} is the static phase. In full-field interferometry the difference in ϕ between two adjacent pixels is a measure of the path length difference $|2\pi|$, which corresponds to $\lambda/2$, where λ is the wavelength of the light source. Thus to demodulate the interferometric signals and obtain $\Delta\phi$ requires an algorithm. The analytic signal of Eq. (1), from a 0th pixel, is ob-

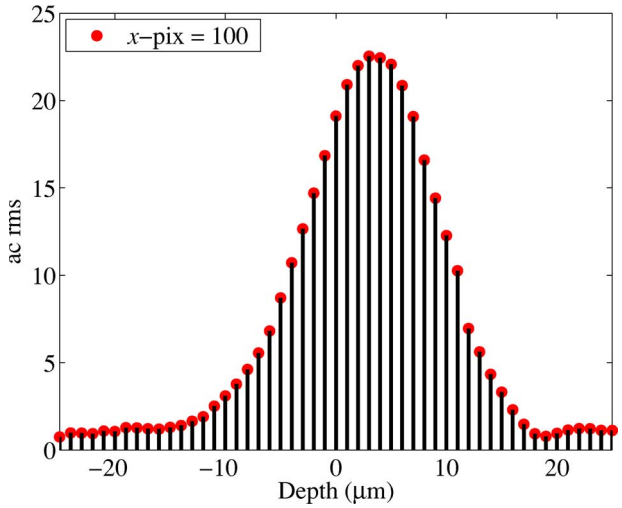

Fig. 3. (Color online) Single digital LCI envelope at the 1.05 mm gauge block. Coherence length of the SLD, $\approx$14 μm; pix, pixel.

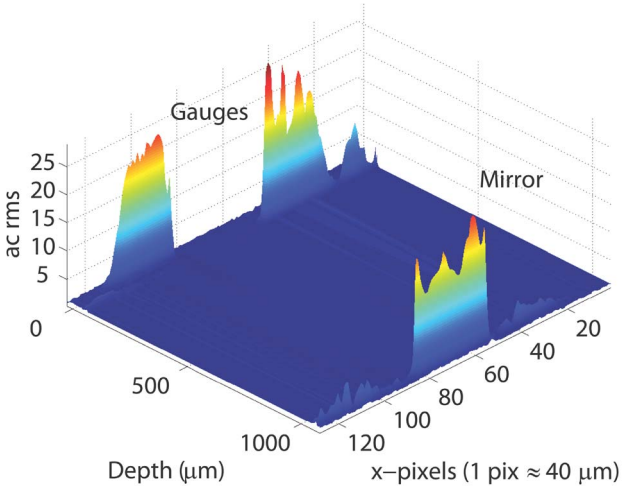

Fig. 4. (Color online) Full-field LCI measurement. Each sample surface can be randomly accessed in depth by digital stepping.

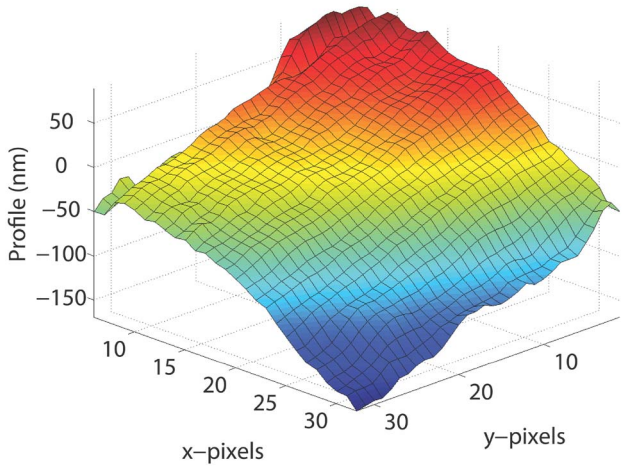

Fig. 5. (Color online) Full-field LCI phase measurement of the 1.05 mm gauge block surface.

tained by application of a bandpass filter with negative frequencies zeroed and is expressed as

$$s_{a0}(t) = \frac{b_0(t)}{2} \exp\{j[2\pi f_c t + \alpha_0(t) + \phi_0]\}. \quad (2)$$

The analytic signal of an adjacent pixel is

$$s_{a1}(t) = \frac{b_1(t)}{2} \exp\{j[2\pi f_c t + \alpha_1(t) + \phi_1]\}. \quad (3)$$

Dividing Eq. (3) by Eq. (2) gives

$$\Phi = \frac{b_1(t)}{b_0(t)} \exp\{j[\alpha_1(t) - \alpha_0(t) + \phi_1 - \phi_0]\}, \quad (4)$$

and the instantaneous phase difference between the two pixels is the argument of Eq. (4), that is,

$$\Delta\phi = \arg(\Phi)_n = [\alpha_1(t) - \alpha_0(t) + \phi_1 - \phi_0], \quad (5)$$

and in the case of spatially uniform temperature changes and translational vibrations $\alpha_1(t) \approx \alpha_0(t)$. Note that $\arg(\Phi)_n$ has an index of sample number, and averaging Eq. (5) over n increases the accuracy of the measurement.

To implement the algorithm outlined above, we built a filter, using the impulse response of a Hanning window convolved with itself in time, and designed it such that the width of the impulse response was equal to four periods of the optical carrier; hence the filtered signal remained relatively insensitive to small carrier frequency fluctuations. The filter impulse response, symmetrical about $t=0$, has the following mathematical expression for $0 \leqslant p \leqslant 1$:

$$h(t) = \left[1 + \frac{1}{2}\cos(2\pi p)\right][1-p] + \frac{3}{4\pi}\sin(2\pi p), \quad (6)$$

where $p = f_c t/2$. The filter passband was centered on the positive carrier frequency by multiplication of the impulse response in Eq. (6) by $\exp(j2\pi f_c t)$. The Fourier transform of the filter impulse response is defined as

$$H(f) = \left[\frac{\sin(\pi q)}{\pi q(q^2-1)}\right]^2, \quad (7)$$

where $q = 2(f - f_c)/f_c$. For $f < 0$, the variable $|q| > 2$ and Eq. (7) is always smaller than 0.003, having a numerical roll-off of $1/f^6$; thus the filter's spectral sidelobes vanish rapidly. Filtering was implemented by time-domain convolution and, using Eqs. (4) and (5), we obtained the phase difference between each pixel and a single reference pixel. The phase map (Fig. 5) of the 32×32 pixel ROI shows the surface of the 1.05 mm gauge block with nanometer resolution. From this measurement, assessment of smoothness and quality of the surface is possible on a scale unobtainable with conventional LCI methods.

To conclude, a new approach to full-field optical metrology has demonstrated random depth access LCI through precise digital stepping and acousto-optic modulation. Furthermore, the technique allows full-field interferometric phase retrieval to be made at random ROIs in depth without electromechanical scanning. Full-field heterodyne LCI provides an inexpensive and functional method of obtaining three-dimensional machine vision. Applications include material surface characterization, microfluidics, and possible adaption to optical coherence tomography.

This project is supported by the University of Limerick Foundation and an Enterprise Ireland International Collaboration grant. The work was undertaken within the framework of a collaboration agreement (18697-2001-11 SOSC ISP IE) between the University of Limerick, Ireland, and the Institute for Health and Consumer Protection, European Commission Directorate General Joint Research Centre, Italy. P. Egan's e-mail address is patrick.egan@ul.ie.

References

1. M. Born and E. Wolf, *Principles of Optics*, 7th ed. (Cambridge U. Press, 1999).
2. H. Matsumoto and A. Hirai, Opt. Commun. **170**, 217 (1999).
3. R. Onodera, H. Wakaumi, and Y. Ishii, Opt. Commun. **254**, 52 (2005).
4. C. K. Hitzenberger and A. F. Fercher, Opt. Lett. **24**, 622 (1999).
5. D. Huang, E. A. Swanson, C. P. Lin, J. S. Schuman, W. G. Stinson, W. Chang, M. R. Hee, T. Flotte, K. Gregory, C. A. Puliafito, and J. G. Fujimoto, Science **254**, 1178 (1991).
6. F. Lakestani, M. P. Whelan, J. Garvey, and D. Newport, in Proc. SPIE **5856**, 23 (2005).
7. P. Egan, F. Lakestani, M. P. Whelan, and M. J. Connelly, in Proc. SPIE **5856**, 427 (2005).